Turkish Journal of Computer and Mathematics Education Vol.12 No.11 (2021), 1015-1024

Research Article

Self-Loosening Failure Analysis Considering Vibration Frequency: Experimental Study for the Spare Tire Carrier

Yohanes T. Wibowo[1]*, Wahyu Irmandi[2], Martinus C. A. Trisnanto[3]

[1]Tool Making Study Program, Astra Manufacturing Polytechnic, Jakarta, Indonesia
[2]Tool Making Study Program, Astra Manufacturing Polytechnic, Jakarta, Indonesia
[3]Tool Making Study Program, Astra Manufacturing Polytechnic, Jakarta, Indonesia
[1]yohanes.trijoko@polman.astra.ac.id

Article History: Received: 11 January 2021; Revised: 12 February 2021; Accepted: 27 March 2021; Published online: 10 May 2021

Abstract: The testing stage involves ensuring a product is produced correctly to achieve the targeted performance. Testing is observed from the determination of looseness resistance for a spare tire carrier to ascertain its durability due to car vibration when driven on flat and bumpy roads to avoid road users' dangers. Therefore, this study was conducted to observe the spare tire carrier's working process and analyze the changes in torque and chain tension in the drive shaft by installing a strain gauge sensor on the chain link. Moreover, the change in strain was converted into tension using mathematical calculations based on test standards. Each component of the spare tire carrier was also analyzed to determine the factors affecting chain tension changes. The results showed that the torque change on the driveshaft was 7.79%, while chain tension was 7.14% on axis 1 and 7.25% on axis 2. Therefore, the spare tire carrier passed the test with the difference not exceeding 25%, which means the road's safety aspect is guaranteed for all the users. However, the new fact is self-looseness is initiated by the vibration due to the stationary engine rotation.

Keywords: Chain Strain; Chain Tension; Looseness Resistance Test; Spare Tire Carrier; Vibration

1. Introduction

The global increase in the human population has promoted more extensive areas to find resources needed by humans [1]. The increase is observed from the transportation required due to the development of broader and more residential areas. The development is necessary because infrastructural development plays a crucial role in mobilizing goods and people in social and commercial activities [2]. Moreover, the addition of road lengths and the emergence of new residential areas have a significant positive impact on economic growth and purchasing power, which further leads to higher mobility [3]. Cars and other transportation modes are, however, used in solving these problems according to geographic conditions. However, they also experience inevitable disruptions both from external and internal factors such as a flat or broken tire. The disruption has led to the addition of spare tires in cars using a special tool known as the spare tire carrier (STC) to anticipate travel disruptions.

This tool is used in tying and keeping a spare tire in a special place in the vehicle when traveling. However, it has also been affected by an existing obstacle loosening its bond due to the vibrations. The vibrations are provided when the engine is started, and the car moves or crosses the road [4, 5]. Loosening is even more intense in a situation the vehicle needs to pass over a bumpy or uneven area apart. This vibration has been reported to be caused by the differences in the level and stability of several variables such as material, surface roughness, tightening strength, tensioning speed, and several tensioning repetitions [6]–[9]. The continuous allowance of this looseness usually increases the possibilities of the spare tire detaching from the carrier, making it very important to road users' safety [10, 11]. Therefore, all STC products are usually tested and confirmed safe, both in function and durability, to prevent such occurrences [12–14].

Modern designs are not focused only on a tool's functionality, which has become an integral part of the design process. Most designs use a finite element method to analyze these tools, but several previous studies found the need to include other methods to obtain good design accuracy. For example, the previous evaluation process showed several things during the manufacturing process that were distorted in the finite element method simulation [15–20].

The vibration frequency changes initiate a looseness due to the displacement produced by the velocity and acceleration changes [6]. It is, however, possible to predict the loosening from the joint shift cycle [4, 5]. Moreover, another study also suggested the suppression or hindrance of loosening through preload and increased friction coefficients and reducing the clamping field's length and tight tolerance [10]. Mo also emphasized the parameters influencing the relaxation, such as the effect of transverse and axial load, bending moment, and friction coefficient on anti-loosening performance [21]. Furthermore, previous research conducted using another STC model has shown that looseness was initiated by vibration [22–24]. The studies were conducted to fill the existing gap on the STC hoist model.

There is the need to test a product after it has been completed, installed, and working in actual conditions. This study, therefore, focused on the looseness resistance test. The test requires several factors due to its complexity. The process involved preparing a jig with sturdy construction and resistance to vibration, followed by the use of a strain gauge for data acquisition. The strain gauge was

used to directly monitor the changes in strain and tension when appropriately placed, after which the data obtained were processed and analyzed [21, 22, 24–31].

A looseness resistance test was conducted in this study through physical simulation in a laboratory using the STC installed on a jig attached to a vibrator machine. Vibrations can be created using different tools such as hammers, piezoelectric, or vibrators with the appropriate tools selected based on structure size, working conditions, and cost [9]. The vibrator machine is responsible for delivering vibrations with patterns and conditions as close as possible to experience when a car is being driven and traveling on the road. The areas of most concern in this research are variations in vibration frequency, repetition, duration, direction, and fatigue or damage, even mechanical failure caused by vibrations [32]. The discussions conducted with silver experts further reinforced the importance of focusing on these aspects. This research was expected to provide a valid model describing the relationship between self-loosening and vibration frequency. Based on that relationship, further, we know the dominant factor initiated the loosening. This research will also provide a looseness resistance test process on the STC hoist in the laboratory to ensure the model's safety [33].

A visual investigation was conducted with a penetrant fluid to determine whether the components cracked or not after the test [34]. The penetrant fluids perform crack checking, a non-destructive test that several researchers have suggested and widely used [35, 36]. These checks confirm the presence or absence of cracks and observe the deformation of the parts in contact as the vibration occurs [37, 38]. The results obtained were analyzed to determine the factors influencing the strain value changes and ascertain the carrier's compliance with the minimum safety standards required. Moreover, the carrier's durability against the looseness due to vibrations caused by outside and those from within, such as the engine, was also evaluated.

The results are expected to be considered by the product development team in improving the design and production of STC. Therefore, this study aimed to obtain a valid testing model related to carrier quality based on the accelerated looseness resistance test, making the product development cycle faster than performing regular tests.

2. Methodology

2.1 Spare Tire Carrier

STC is a car part that binds, holds, ties, and keeps the spare tire in place wherever the vehicle is traveling. It is mainly located under the body, in the trunk, or attached to the car's back, with some of the available types being hoist (chain), clamp, and bun. However, this study focused on the hoist type located at the bottom of the car, as shown in figure 1. It has a hanging plate that helps in positioning and serves as a buffer for the spare wheel, hoisted until it touches the cross-member surface.

Figure 1: Spare tire carrier – hoist type

2.2 Stress and Strain

Stress compares the working force and the cross-sectional area of an object, while a strain is defined as the ratio between the increase in the current and initial lengths. Meanwhile, Modulus Elasticity or Young's Modulus (E) is the ratio between the stress and strain of an object and calculated using the following equation after the strain and length gain equations have been substituted [39].

$$E = \frac{FxLo}{AxΔL} \quad (1)$$

2.3 Looseness Resistance and Procedure Tests

Looseness Resistance Test (LRT) involves the vibration of the jig, spare tire, and STC in the vertical direction (z-axis) using a vibration testing machine. LRT was used to determine the STC's resistance in binding the spare tire against looseness caused by vibration when the engine starts and the period the car is being driven on a flat or bumpy road. The parameters determined include the changes in the values of torque on the driveshaft and the chain tension.

This looseness resistance test procedure is usually based on the object's function's standards to be tested. In the pre-test position, the tires were hoisted to the cross member's touch and tightened according to the 38.5 Nm standard. The actual test was conducted for 60 minutes with a tire pressure of 300 Kpa. The vibration direction was placed vertically or parallel to the z-axis at a vibration frequency of 10 - 42 Hz and acceleration of 1G or 9.8 m/s2. Meanwhile, the evaluation standard involved the reduction in torque and chain tension not exceeding 25% and observing no cracks in all STC components even with deformation allowance.

2.4 Dye Penetrant Inspection

Dye penetrant inspection is one of the Non-Destructive Test (NDT) visual inspection methods used in detecting defects on open surfaces of solid components, both metal and non-metal. It is used to obtain a clearer view of the material's defects using the test object and 1 set of dye penetrant fluid, including the cleaner, penetrant, developer, and cloth. The visual method was also used in observing the deformation in the components of the vibration.

2.5 Strain Gauge

A strain gauge is a sensor attached to the specimen surface to measure the strain occurring due to physical deformation caused by stress. This instrument's main component is a thin metal foil grid that serves as a resistive conductor coated with a pair of protective membranes and an insulator, as shown in figure 2. It also has an isolator that helps in gluing the strain gauge to the measuring plane. This instrument's working principle is such that the resistance value on the strain gauge changes linearly when there is a strain on the specimen. A 2-axis round base type has an impedance of 120 Ω, a gauge factor of 2.00 ± 1.0%, and adhesive glue CC-33A, EP-340 was used for the steel in this study.

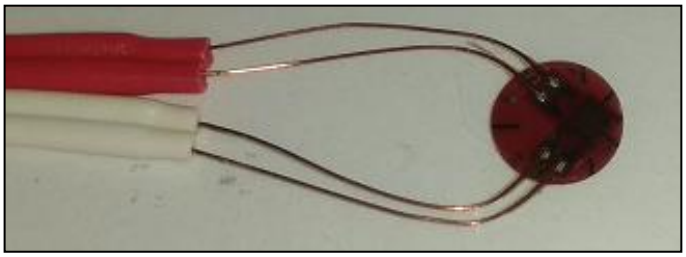

Figure 2: Strain gauge round base 2 axis

The resistance change was evaluated by multiplying the values of initial resistance, gauge factor, and strain. Meanwhile, another function closely related to a strain gauge is the Wheatstone Bridge which is an arrangement of electrical circuits in a bridge box used in measuring the value of an unknown resistance by equating the voltage flowing on the galvanometer to zero due to the equality of the potential edges. However, the receiver of a different resistance from the strain gauge installed in one of the Wheatstone Bridge circuits causes a change in the voltage on the galvanometer, which is calculated using the following equation [40].

$$v=1/4 \text{ x } ΔR/R \text{ x } v' \quad (2)$$

Where v 'is the excitation voltage, ΔR is the change in resistance, R is the initial resistance, and v is the output voltage.

2.6 Research Framework

This study started with a literature study while data collection was used to select an instrument. The looseness was tested, followed by analysis and evaluation to answer the research questions formulated at the beginning of

the research.

2.7 Product Data

STC consists of 6 components, including the main body, which serves as the home for the others: driveshaft, gear wheel, pinion gear, chain guide, and chain. The drive shaft serves as a drive for the pinion gear and gear wheel and an adapter for the jack handle. The gear wheel functions as the STC chain's main driver, while the pinion gear serves as the STC chain's main driver. Meanwhile, the chain guide is the chain positioner when it is moved up and down, while the chain is the hanging plate puller to hold the spare tire. Moreover, the hanging plate acts as a support and positioner for the spare tire when it is tightened.

2.8 Data Acquisition System

Data Acquisition System (DAS) is the device used in the process of retrieving test data. It consists of sensors such as a strain gauge that receives input in the form of physical phenomena in the test area and data acquisition hardware and software used in displaying the results of the data recorded to the monitor. An LMS Scadas Recorder was used in this study.

2.9 Jig Looseness Resistance Test and Testing Machines

The test was conducted in the Testing and Durability (TND) department according to customer requests. Therefore, a special jig suitable for the existing test specimens and test machines was required, as shown in Figure 3.

 esistance test

The STC, spare tires and jigs were placed on top of a vibratory engine that can withstand the entire installation load for the LRT. Meanwhile, the vibration machine used was an IMV model EM2502 with a frequency range of 5 - 2500 Hz, a maximum payload of 500 kg, a load capacity of 40000N, and the ability to vibrate on both horizontal and vertical axis.

3. Results and discussion

3.1 Testing Preparation

Almost all the components and measuring instruments used in this study were made of iron, with the surface quality being the most important parameter [41, 42]. Therefore, they were carefully prepared and checked to ensure they are in good condition without any visual defect. This visual method has been widely used in the metal industry [43, 44].

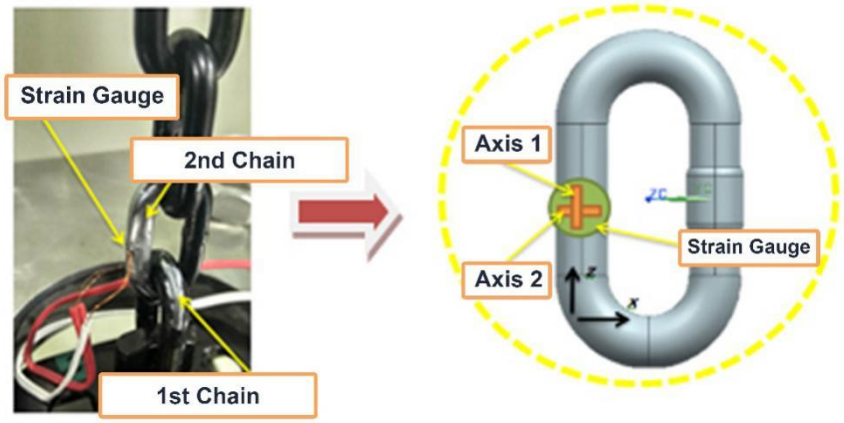

Figure 4: The installation of strain gauge on the chain

The strain gauge position is a critical success and accuracy factor in the monitoring and data collection process [45–47]. However, particular attention is required to determine the optimum location to install the strain gauge in the area considered deformed [48, 49]. Moreover, a strain gauge was attached to the second link from the bottom to simplify the checking process. At the same time, chain fitting was included in the high-precision measurement category due to its ability to provide values with the lowest uncertainty degree [50]. The installation on the second chain also considered the limited space, as shown in Figure 4. The spare tire was filled with air at a maximum of 300 Kpa before the STC was installed on the jig, which means the setup resembled the actual conditions [51, 52].

Furthermore, the spare tire was also raised to have a forward slope of 8°. Simultaneously, the final stage involved tightening the drive shaft using a torque wrench. This also tightened the chain, thereby distributing force and triggering the sensor to read the strain gauge length change. A torsion meter was also crucial to obtaining good results for repeatable and reliable measurements, while the measurement of torque is essential and fundamental to all rotating joints [53].

The STC, jig, and spare tire were installed on top of the vibration machine, while an accelerometer/vibration sensor was installed on the tires, cross members, and upper frame of the jig to determine each part's frequency. The accelerometer served as a reference for engine vibration during the test due to its ability to represent the vehicle chassis' vibrations. At the same time, other sensors were used to provide supporting data.

3.2 Testing

The test was conducted with a jig, spare tire, and STC, which were vibrated in the direction of the vertical axis (z-axis) using a vibration testing machine with the frequency varied between 10 Hz and 42 Hz to determine the most significant vibration magnitude and different effects [54, 55]. The frequency was varied constantly at a duration of 5 minutes, repeatedly for 60 minutes. This is in line with the sufficiently good duration determined in previous studies to obtain a loosening cycle above 100 [56, 57]. Meanwhile, the vibration acceleration used was 1G (9.81m/s2).

3.3 Testing Result

The main parameters that determined whether the specimen passes the LRT test include the torque change's magnitude on the driveshaft and the chain tension. The following results were, therefore, obtained from the test.

3.3.1 Change in torque on the driveshaft

A change was observed in the torque on the drive shaft after the test, with the initial value recorded to be 385 Kgf.cm while the post-test measurement was 355 Kgf.cm, which means there is a change of 30 Kgf.cm or approximately 7.79%.

3.3.2 Chain strain changes

Two-axis strain gauges were installed on the STC chain to measure the vertical and horizontal changes in strain.

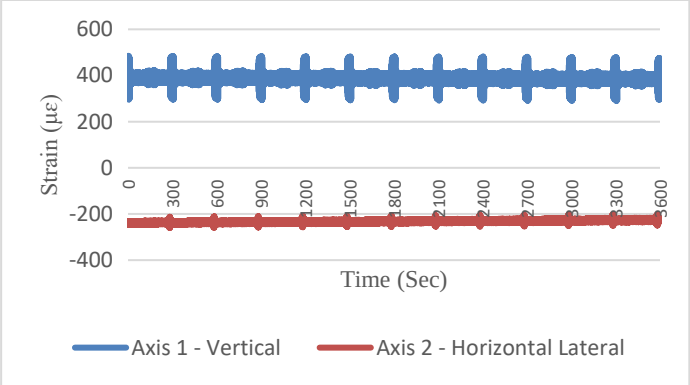

Figure 5: Strain and time graph

Figure 5 shows the strain on axis 1 or vertical axis decreased by 27.72 με, and this was observed from the values before and after the test, which was 388.02 με and 360.3 με respectively. Meanwhile, axis 2 or horizontal axis had an increase of 17.77 με based on the values before and after the test, which were -236.63 με and -219.47 με respectively. Moreover, Figure 6 shows the change in strain difference due to dynamic conditions such as the mechanical vibrations accompanied by the noise, which disturbs the measurement signal.

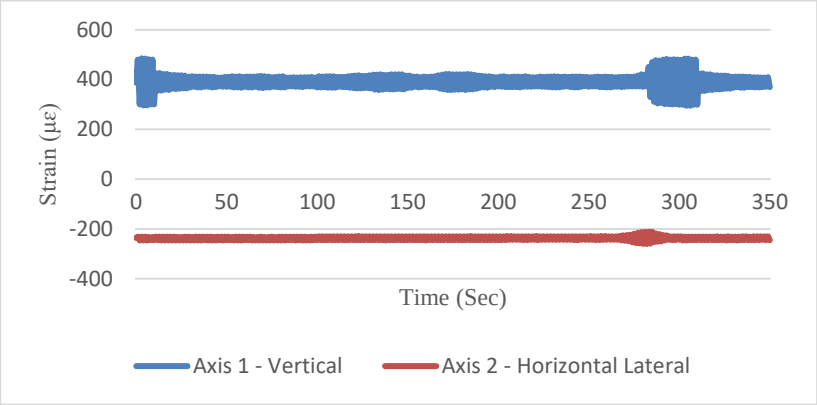

Figure 6: Strain and timing details

3.4 Analysis of Test Results

According to the standard, changes in chain tension are required to be included in the report. Therefore, it is necessary to convert from chain strain to chain tension in Newton (N) units using the elasticity modulus and stress-strain equation. The results are shown in the following Table 1.

Table 1: Floating-point operations necessary to classify a sample

Measurement Time	Direction	Strain (uε)	Tension (Mpa)	Tensile Stress (N)	Deviation (N)	Percentage
Before Test	Axis 1	388.02	81.48	3301.42	-	-
	Axis 2	-236.63	49.56	-2013.34	-	-
After Test	Axis 1	360.30	75.60	3065.57	235.85	7.14 %
	Axis 2	-219.47	45.99	-1867.33	-146.01	7.25 %

Table 1 shows the difference in chain tension measurement on axis 1 and axis 2 before and after the test was 235.85 N on axis 1 and -146.01 N on axis 2. The table represents by 7.69% and 7.81%, respectively. The 30 Kgf.cm torque change on the driveshaft indicates loosening by vibration. This situation is in line with the findings of Hao and Syed. It is very dangerous to leave the driveshaft unchecked since the possibility of causing unsafe conditions in the form of mechanical failure [4, 5, 32]. The finite element analysis was conducted on a technical basis during the STC design stage to determine the continuation of the detailed design and manufacturing stage. However, the loosening incident strengthens the opinion that distortion occurs during the manufacturing process, as Weiland stated [16]. It also confirms that the finite element method is insufficient, which means the real test is required [18–20]. Furthermore, the results also corroborate Linbo's research that changes and acceleration of vibrational frequencies also contribute to loosening, as observed with the contribution of 1G. Further observations need to be conducted to determine the level of the contribution and limit of acceleration due to its probable effect [6].

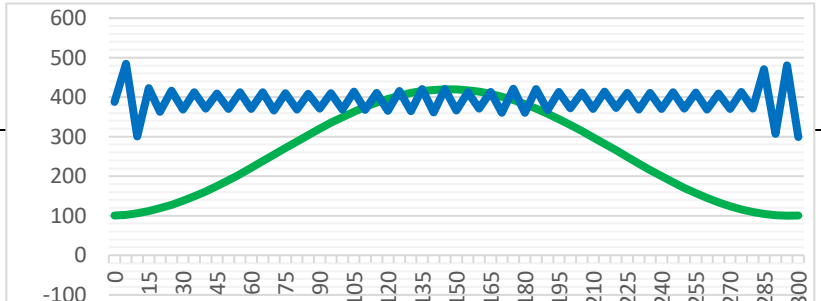

Figure 7: Strain and Frequency (10x)

Figure 7 fully describes the relationship between chain strain, time, and frequency. For clarity, the frequency is shown as 10x the original frequency. The maximum vertical strain occurs in the initial 10 seconds, where the frequency starts the vibration. In the first 10 seconds, STC vibrated with a frequency of 10.04 - 10.62 Hz, then at 15 seconds, the vertical strain began to be consistently average, and STC vibrated at a frequency of 11.17 Hz. In the last 20 seconds of the frequency sinusoidal cycle, as the vibration approaches the frequency of 10 Hz, the vertical strain again increases to the maximum.

In summary, it can be stated that at the vibration frequency around 10-11 Hz, there is an increase in the maximum strain up to 60 με. The 10-11 Hz frequency will occur when the car engine rotates at a speed of 600-660 rpm from the calculation and measurement. At a frequency of 11.5 Hz, the car engine will rotate at 690 rpm. This fact shows that the design has been made correctly and has taken into account engine vibration, but the engine rotation's vibration convincingly causes the self-looseness itself. Usually, car manufacturers set stationary engine speeds to be around 700 rpm with a -50 to +50 rpm tolerance.

After the test, the STC was dismantled to investigate each component to ascertain the presence or absence of cracks and the cause of the chain tension changes. This investigation was conducted by spraying a penetrant liquid. The results showed the main body, chain guide, chain and hanging plate, driveshaft, gear wheel, and pinion gear components did not experience a crack, but the pinion gear component was deformed at the gear tip. These findings corroborated Chowdhury and Bhuiyan's research that one of the vibration effects is deformation [37, 38]. Therefore, the literature review, discussion, and investigation showed the deformation was due to the difference in hardness between the gear wheel and pinion gear. The material's hardness is also closely related to the strain rate inherent in its properties [58]. The gear wheel was made of cast iron with a 68 HRc, while the pinion gear was made of SPHC 270 with 31 HRc. Meanwhile, when the STC is vibrated, the pinion gear rubs directly against the gear wheel. The friction causes deformation, which is indicated by the wear's appearance on the gear tip, which further leads to loosening in the STC bond, as shown in Figure 8.

Figure 8: Deformation of the pinion gear

At the initial level, the deformation or wear does not reduce tool performance but contributes to looseness's appearance at a particular stage, as stated in previous research. This condition's allowance makes the looseness due to deformation occur much earlier and much more dangerous than those observed due to chain tension changes.

4. Concl u s ion

This study was conducted using several mathematical calculations, and the results showed there is a change of 30 Kgf.cm or 7.79% in the torque on the driveshaft and 235.85 N or 7.14% and -146.01 N or 7.25% in the chain tension on axis 1 or vertical axis and 2 or horizontal axis respectively. Moreover, the difference observed before and after the test was found not to pass the allowable threshold of 25%, and this shows the STC passed the looseness resistance test. The result means the loosening is within the normal limits. However, one new fact is that the initiator of self-looseness in STC is the vibration due to stationary engine rotation. The engine's stationary rotating speed, which is in the range of 650-750 rpm, produces a vibration frequency of 10-11 Hz, which causes maximum vertical strain. The previous investigations performed visually with penetrant fluids' aid showed no crack in all STC components. The deformation of the pinion gear was caused by the differences in the hardness of the material. It is essential to focus on this aspect because it can be a source of the decline in STC performance and function and in initiating loosening. This research showed the loosening attenuation test had not been reached by utilizing the tightness of tolerance, and the contribution of manufacturing distortion to loosening was not determined. These two conditions are closely related due to their occurrence in the component manufacturing process. This means it is possible to improve the finite element method using conditions considered closer to reality to minimize the use of a real tool for testing. It is suggested that further research simultaneously attach strain gauge to the other links to obtain a more representative picture of the changes in length and observe the homogeneity of the chain material.

5. Acknowledgments

The authors are grateful to Astra Manufacturing Polytechnic for their great discussions and support. The authors are also grateful to PT. Astra Otoparts, Tbk as an industry partner for great research collaborations.

References

1. L. Wang and L. Chen, “The impact of new transportation modes on population distribution in Jing-Jin-Ji region of China,” *Sci Data*, vol. 5, no. 1, p. 170204, 2018.
2. C. Ng, T. Law, F. Jakarni, and S. Kulanthayan, “Road infrastructure development and economic growth,” *IOP Conf Ser Mater Sci Eng*, vol. 512, p. 12045, 2019.
3. C. P. Ng, T. H. Law, S. V. Wong, and S. Kulanthayan, “Relative improvements in road mobility as compared to improvements in road accessibility and economic growth: A cross-country analysis,” *Transp Policy*, vol. 60, pp. 24–33, 2017.
4. Y. X. Nassar S.A., “Modeling the Effect of Nut Thread Profile Angle on the Vibration-Induced Loosening of Bolted Joint Systems,” in *Advanced Joining Processes. Advanced Structured Materials, Vol 125*, L. da Silva, P. Martins, and M. El-Zein, Eds. Singapore: Springer, 2020, pp. 29–54.
5. H. Gong, J. Liu, and X. Ding, “Thorough understanding on the mechanism of vibration-induced loosening of threaded fasteners based on modified Iwan model,” *J Sound Vib*, vol. 473, p. 115238, 2020.
6. L. Zhu, J. Hong, G. Yang, and X. Jiang, “Experimental study on initial loss of tension in bolted joints,” *Proc Inst Mech Eng Part C J Mech Eng Sci*, vol. 230, no. 10, pp. 1685–1696, Apr. 2015.
7. Z. Juanqing, J. Yingjie, L. Lishun, X. Gengjie, and S. Yanlin, “Optimization and improvement of hydraulic system of retracting and extending devices of spare wheel carrier,” *Hoisting Conveying Mach*, vol. 7, 2015.
8. P. Chao, “Optimization Research of Structure of Spare Tire Rack Basaed on Solidwork Motion,” *Spec Purp Veh*, vol. 1, 2017.
9. S. M. Y. Nikravesh and M. Goudarzi, “A Review Paper on Looseness Detection Methods in Bolted Structures ,” *Latin American Journal of Solids and Structures* , vol. 14. scielo , pp. 2153–2176, 2017.
10. Z. Wang *et al.*, “Clamp looseness detection using modal strain estimated from FBG based operational modal analysis,” *Measurement*, vol. 137, pp. 82–97, 2019.
11. H. Gong, J. Liu, and X. Ding, “Study on the critical loosening condition toward a new design guideline for bolted joints,” *Proc Inst Mech Eng Part C J Mech Eng Sci*, vol. 233, no. 9, pp. 3302–3316, Sep. 2018.
12. M. Z. Sadeghi *et al.*, “Damage detection in adhesively bonded single lap joints by using backface strain: Proposing a new position for backface strain gauges,” *Int J Adhes Adhes*, vol. 97, p. 102494, 2020.
13. G. Yang, C. Che, S. Xiao, B. Yang, T. Zhu, and S. Jiang, “Experimental Study and Life Prediction of Bolt Loosening Life under Variable Amplitude Vibration,” *Shock Vib*, vol. 2019, p. 2036509, 2019.
14. S. Ling, Z. Huagang, and W. Tao, “Offset spare wheel carrier failure analysis and improvemenT,” *Automob Appl Technol*, vol. 6, 2016.
15. P. Danielczyk and J. Stadnicki, “Reconstruction of the Main Cylinder of Carding Machine-Optimization of Dimensions with the Use of the Finite Element Method,” *Arch Mech Eng*, vol. LIX, Jan. 2012.
16. J. Weiland, M. Z. Sadeghi, J. V Thomalla, A. Schiebahn, K. U. Schroeder, and U. Reisgen, “Analysis of back-face strain measurement for adhesively bonded single lap joints using strain gauge, Digital Image

Correlation and finite element method," *Int J Adhes Adhes*, vol. 97, p. 102491, 2020.
17. A. C. Isaacson, *The Design and Constructionof a Rear Bumper with Incorported Spare Tire Rack*. San Luis Obispo: California Polytechnic State University, 2016.
18. A. I. Karayan, D. Ferdian, S. Harjanto, D. M. Nurjaya, A. Ashari, and H. Castaneda, "Finite Element Analysis Applications in Failure Analysis: Case Studies," InTech Open, 2012, pp. 217–234.
19. E. Marques, F. Silva, and A. Pereira, "Comparison of Finite Element Methods in Fusion Welding Processes—A Review," *Met 2020*, vol. 10, no. 75, 2020.
20. J.-D. Caprace, G. Fu, J. F. Carrara, H. Remes, and S. B. Shin, "A benchmark study of uncertainness in welding simulation," *Mar Struct*, vol. 56, pp. 69–84, 2017.
21. Y. Mo, S. Guo, X. Qin, J. Qin, K. Zhan, and X. Gao, "Research on the Numerical Calculation Method for Antiloosening Performance of Screwed Joints under Complex Working Conditions," *Math Probl Eng*, vol. 2020, p. 5915173, 2020.
22. N. K. A. Utomo and L. Anggraini, "Finite Element Analysis With Static And Dynamic Conditions Of Spare Wheel Carrier For Oh 1526 Fabricated By Saph 440 Hot Rolled Steel," *J Mech Eng Mechatronics*, vol. 4, no. 1, pp. 34–44, 2019.
23. K. Shete, "Advanced Spare Wheel Carrier," *Int J Sci Eng Res*, vol. 6, no. 7, pp. 828–832, 2015.
24. P. Chao, L. Lishun, and L. Hngxun, "ADAMS based parametrized modeling and optimization design of spare tire release and retract device," *Hoisting Conveying Mach*, vol. 10, 2017.
25. . C. Thakare, S. H. Limaye, B. S. Babu, K. Kumar, T. V. Vardhan, and S. S. Kumar, "Design and development of test setup for impact endurance test on chain tensioner," *AIP Conf Proc*, vol. 2200, no. 1, p. 20023, Dec. 2019.
26. Y. Chen, Q. Gao, and Z. Guan, "Self-Loosening Failure Analysis of Bolt Joints under Vibration considering the Tightening Process," *Shock Vib*, vol. 2017, p. 2038421, 2017.
27. K. Zhou and Z. Y. Wu, "Strain gauge placement optimization for structural performance assessment," *Eng Struct*, vol. 141, pp. 184–197, 2017.
28. A. Mesic, M. Colic, E. Mesic, and N. Pervan, "Stress Analysis of Chain Links in Different Operating Conditions," *Int J Eng Sci Invent*, vol. 5, no. 12, pp. 43–49, 2016.
29. H. Moayedi, R. Nazir, M. Gör, K. Anuar Kassim, and L. Kok Foong, "A new real-time monitoring technique in calculation of the p-y curve of single thin steel piles considering the influence of driven energy and using strain gauge sensors," *Measurement*, vol. 153, p. 107365, 2020.
30. V. S. Ignakhin, V. S. Severikov, and A. M. Grishin, "Tensile and torsional strain gauge based on Fe48Co32P14B6 metallic glass," *J Magn Magn Mater*, vol. 476, pp. 382–386, 2019.
31. X. Zhang, W. Li, Z. Zhu, W. Ren, and F. Jiang, "Tension monitoring for the ring chain transmission system using an observer-based tension distribution estimation method," *Adv Mech Eng*, vol. 9, no. 9, p. 1687814017727251, Sep. 2017.
32. N. S. Ahirrao, S. P. Bhosle, and D. V Nehete, "Dynamics and Vibration Measurements in Engines," *Procedia Manuf*, vol. 20, pp. 434–439, 2018.
33. F. Y. Cavdar *et al.*, "Setup for testing the vibration-based loosening of pre-loaded bolted joints," *Mater Test*, vol. 61, no. 10, pp. 981–985, Oct. 2019.
34. Y. Kadin, M. Mazaheri, V. Zolotarevskiy, C. Vieillard, and M. Hadfield, "Finite elements based approaches for the modelling of radial crack formation upon Vickers indentation in silicon nitride ceramics," *J Eur Ceram Soc*, vol. 39, no. 14, pp. 4011–4022, 2019.
35. M. Schröder, C. Biedermann, and R. Vilbrandt, "On the applicability of dye penetrant tests on vacuum components: Allowed or forbidden?," *Fusion Eng Des*, vol. 88, no. 9, pp. 1947–1950, 2013.
36. K. Manikandan, P. Sivagurunathan, S. Ananthan, A. Moshi, and S. Bharathi, "Study on the influence of temperature and vibration on indications of liquid penetrant testing of A516 low carbon steel," in *Materials Today*, 2020.
37. M. Chowdhury, "The effect of frequency of vibration and humidity on the coefficient of friction," *Tribol Int - TRIBOL INT*, vol. 39, pp. 958–962, Sep. 2006.
38. M. S. H. Bhuiyan and I. A. Choudhury, "Investigation of Tool Wear and Surface Finish by Analyzing Vibration Signals in Turning Assab-705 Steel," *Mach Sci Technol*, vol. 19, no. 2, pp. 236–261, Apr. 2015.
39. L. Negi, *Strength of Material*. New Delhi: Tata McGraw Hill Education Private Limited, 2010.
40. Kyowa, *What is a Strain Gauge*. Tokyo: Kyowa Electronic Instrument Co, 2005.
41. N. Neogi, D. K. Mohanta, and P. K. Dutta, "Review of vision-based steel surface inspection systems," *EURASIP J Image Video Process*, vol. 2014, no. 1, p. 50, 2014.
42. X. Sun, J. Gu, S. Tang, and J. Li, "Research Progress of Visual Inspection Technology of Steel Products-A Review," *Appl Sci*, vol. 8, no. 2195, 2018.
43. X. Kong and J. Li, "Image Registration-Based Bolt Loosening Detection of Steel Joints," *Sensors (Basel)*, vol. 18, no. 4, p. 1000, Mar. 2018.
44. X. Kong and J. Li, "Vision-Based Fatigue Crack Detection of Steel Structures Using Video Feature

Tracking," *Comput Civ Infrastruct Eng*, vol. 33, no. 9, pp. 783–799, Sep. 2018.
45. A. Kumar, S. Chaturvedi, V. Chaturvedi, and R. Yadaw, "Design Studies and Optimization of Position of Strain Gauge," *Int J Sci Eng Res*, vol. 3, pp. 1–4, Oct. 2012.
46. A. Kumar, V. Chaturvedi, and S. Chaturvedi, "Optimization of Position of Strain Gauge Using Geometrical Parameter of Sensor's Subtrate," *VSRD Int J Mech Automob Prod Eng*, vol. 2, no. 7, pp. 263–268, 2012.
47. J. Juraszek, "Strain and force measurement in wire guide," *Arch Min Sci*, vol. 63, pp. 321–334, Jan. 2018.
48. M. Pastor, F. Trebuna, P. Lengvarsky, and J. Bocko, "Possibility of Using of Tensometry in Deformation Analysis in Areas With Sudden Change of Geometry," *Am J Mech Eng*, vol. 4, no. 7, pp. 363–367, Dec. 2016.
49. Y. Xia, J. Zhu, K. Wang, and Q. Zhou, "Design and verification of a strain gauge based load sensor for medium-speed dynamic tests with a hydraulic test machine," *Int J Impact Eng*, vol. 88, pp. 139–152, 2016.
50. A. Schafer, "New Strain gauge-based torque reference chain offering smallest measurement uncertainties," in *19th International Congress of Metrology*, 2019, pp. 1–6.
51. J. Popat *et al.*, "A Statistical Study of Tire Pressures on Road Going Vehicles," *SAE Int J Passeng Cars - Mech Syst*, vol. 9, no. 2, pp. 560–564, 2016.
52. A. Elfasakhany, "Tire Pressure Checking Framework: A Review Study," *Reliab Eng Resil*, vol. 1, no. 1, pp. 12–28, 2019.
53. J. Goszczak, "Torque measurement issues," *IOP Conf Ser Mater Sci Eng*, vol. 148, p. 12041, 2016.
54. SKF, *Vibration Diagnostic Guide*. San Diego, California: SKF Reliability Systems, 2000.
55. Valmet, "Vibration Analysis." Valmet Technical Paper Series, p. 13, 2011.
56. S. Hashimura and D. F. Socie, "A Study of Loosening and Fatigue of Bolted Joints under Transverse Vibration." SAE International , 2005.
57. Y. Jiang, M. Zhang, and C.-H. Lee, "A Study of Early Stage Self-Loosening of Bolted Joints," *J Mech Des - J MECH Des*, vol. 125, Sep. 2003.
58. E. Evin and M. Tomáš, "Comparison of Deformation Properties of Steel Sheets for Car Body Parts," *Procedia Eng*, vol. 48, pp. 115–122, 2012.